PAPER

Revealing the *in situ* NaF generation balance for user-friendly controlled synthesis of sub-10 nm monodisperse low-level Gd^{3+}-doped β-NaYbF$_4$:Er†

Ji-Wei Shen, [ID] * Zhiqing Wang, [ID] Xiaoxuan Wei, Jiawei Liu [ID] and Yinmao Wei [ID] *

Herein, user-friendly control of the synthesis of sub-10 nm hexagonal (β-) NaYbF$_4$:Er nanocrystals (NCs) with extremely low-level Gd^{3+} doping (0%, 10 mol%) was achieved. We reveal for the first time that the effective sodium/fluoride levels during the formation of cubic (α-) nuclei are not only controlled by the sodium/fluoride to rare-earth precursor ratios used, but also sensitively restricted by the *in situ* NaF generation reaction in a sodium oleate-based solvothermal system. Excessive *in situ* NaF generation will lead to a respective sodium- and fluoride-deficient environment, delayed α-to-β transition and larger β-NCs. Based on these effects, sub-10 nm monodisperse low-level Gd^{3+}-doped β-NaYbF$_4$:Er was obtained with a user-friendly low fluoride dosage by finely balancing this NaF generation reaction and achieving an intrinsic optimized sodium-fluoride level for NC nucleation. Notably, our work represents the first example where the focus is on the competing *in situ* NaF generation reaction and its use for nucleation regulation, as well as for the user-friendly control of the solvothermal synthesis of sub-10 nm β-NaYbF$_4$:Er.

Introduction

The controlled synthesis of multifunctional rare-earth upconversion nanocrystals (UCNCs) is useful for various applications.[1-6] As a facile strategy, Gd^{3+} doping could provide synergistic controlled synthesis and multiple functionalities for promising UCNCs obtained *via* the solvothermal method, especially for β-NaYbF$_4$-based materials.[7-10] The sodium and fluoride sources in the solvothermal synthesis of Gd^{3+}-doped β-NaYbF$_4$ are generally supplied by a methanolic solution containing NaOH and NH$_4$F according to a typical optimal sodium/fluoride/rare-earth (Na/F/RE) ratio of 2.5 : 4 : 1.[11] When the molar doping ratio of Gd^{3+} reaches as high as 30% and 40%, the diameter of the Gd^{3+}-doped β-NaYbF$_4$ particles is ~20 nm and ~12 nm, respectively. However, the particle diameters are still as high as ~80 nm and ~44 nm when the molar doping ratios of Gd^{3+} are 10% and 20%, respectively.[9,10] It is highly desirable to achieve sub-10 nm β-NaYbF$_4$ by using low-level Gd^{3+} doping (*e.g.*, 0% or 10%), which may be more favorable for high upconversion efficiency.

Insights into the intrinsic UCNC nucleation process should provide new strategies that can overcome the above synthesis control issues. Surveying the literature, we noticed that the previous solvothermal nucleation investigations were mainly

Key Laboratory of Synthetic and Natural Functional Molecule Chemistry of the Ministry of Education, College of Chemistry & Materials Science, Northwest University, Xi'an 710069, China. E-mail: jiweish@nwu.edu.cn; ymwei@nwu.edu.cn

focused on regulating the nucleation time, solvent compositions and Na/F/RE ratio from a macroscopic viewpoint.[12-14] For achieving small-sized β-UCNCs, sodium oleate (NaOA) used as a sodium source has recently shown its attractively superior properties compared to the most often used NaOH sodium source. Haase and co-workers pioneered the α-nucleus composition *versus* Na/RE ratio investigations and achieved an efficient NaOA-based solvothermal UCNC controlled synthesis strategy.[14,15] However, the Na/RE ratio control in their work was also conducted from the macroscopic point of view. A high Na/F/RE ratio (*e.g.*, 8 : 11 : 1) that was far in excess of the typical value of 2.5 : 4 : 1 was essential for achieving α-nuclei with a high sodium content in order to obtain a fast α-to-β transition and small-sized β-UCNCs according to their strategy. The formation of sodium-deficient α-nuclei under a low Na/F/RE ratio of 2 : 5 : 1 was unreasonable to some degree because such a ratio was close to the typical value of 2.5 : 4 : 1. The same high Na/F/RE ratio of 8 : 11 : 1 was also used for the preparation of sub-10 nm β-NaYbF$_4$:Tm, and reagent-consuming synthesis was seemingly unavoidable for sub-10 nm β-NaYbF$_4$.[16] The intrinsic reasons for the variations in the number of β-nuclei and the UCNC controlled synthesis effects *via* variation of the Na/F/RE ratio are still unclear.[14,16]

Fine-tuning of the intrinsic sodium/fluoride levels, as well as their functional morphologies, and the resultant impacts on α-nuclei and β-UCNC formation appear to have been overlooked somewhat in the past. Recently, we achieved small-sized β-NaYbF$_4$:Er (~11.0 nm) with a size close to 10 nm by using a NaOA-based solvothermal strategy, but with a low level of sodium and fluoride sources (NaOA/F/RE, 2.5 : 4 : 1).[17] Such small-sized β-

NaYbF$_4$:Er was formed due to low *in situ* NaOA/NH$_4$F-to-NaF conversion reactivity but enhanced NH$_4$F-to-HF decomposition reactivity. We can imagine that the high Na/F/RE ratio (*e.g.*, 8 : 11 : 1)-based solvothermal systems described in the literature will provide not only a large amount of *in situ* generated NaF, but also the user-unfriendly HF. The UCNC nucleation process actually consists of two separate but competing reactions of NaF generation and α-nuclei formation. To date, this *in situ* NaF generation reaction has received almost no attention in UCNC controlled synthesis. Our motivation was thus to achieve the user-friendly control of the synthesis of sub-10 nm low-level Gd^{3+}-doped β-NaYbF$_4$:Er by using a low Na/F/RE ratio.

In this work, the definite competing reactions of *in situ* NaF generation and α-nuclei formation during NaOA-based solvothermal UCNC nucleation were proposed. In contrast with the typical highly skewed NH$_4$F/RE ratio optimization process (*e.g.*, from 4 : 1 to 8 : 1), we revealed for the first time that fine-tuning of the NH$_4$F/RE ratio in the vicinity of the stoichiometric value could sensitively balance the competing *in situ* NaF generation reaction during NaOA-based solvothermal α-nuclei formation and thus achieve user-friendly and reagent-saving control of the synthesis of sub-10 nm low-level Gd^{3+}-doped β-NaYbF$_4$:Er by using a very low Na/F/RE ratio.

Experimental

Materials

All chemicals used were of at least analytical grade. Oleic acid (HOA, technical grade, 90%), 1-octadecene (ODE, technical grade, 90%), sodium oleate and rare-earth acetates were obtained from Sigma-Aldrich (St. Louis, MO, USA). Ammonium fluoride (NH$_4$F, 98%) was purchased from Aladdin Industrial Corporation (Shanghai, China).

Fine tuning of the sodium/fluoride level for NaOA-based solvothermal controlled synthesis of NaYbF$_4$:Er (2 mol%)

The synthesis procedures were performed according to the NaOA-based solvothermal strategy for the preparation of UCNCs reported in the literature with some modifications.[18] A mixed solution of HOA/ODE (3.6 mL/9 mL) was added to a three-necked flask containing the corresponding 0.6 mmol of rare-earth acetates. A heating procedure (160 °C for 30 min) was then performed to obtain rare-earth oleates. On cooling down to 35 °C, NaOA (1.5 mmol) was introduced into this system, followed by stirring at this temperature for 10 min. The designed amount of NH$_4$F dissolved in methanol was then added, followed by stirring at 35 °C for 30 min and an increase in the system temperature to 100 °C. The system was cooled down naturally after final UCNC growth at 300 °C.

The as-obtained NaYbF$_4$:Er was purified and re-dispersed in cyclohexane, and the insoluble component was isolated *via* centrifugation prior to product characterization. The X-ray powder diffraction (XRD) results indicated that NaF comprised the majority of the insoluble component. The mass of the insoluble component was thus used to reflect the NaF content of the system.

To achieve a reagent-saving controlled synthesis strategy for sub-10 nm β-NaYbF$_4$:Er, unless otherwise specified, the Na/RE ratio was kept constant at 2.5 : 1 in this work.

Monitoring of the NaF level during solvothermal synthesis

The solvothermal reactions were stopped by rapid cooling with the help of cool air flow. NaF was collected *via* washing the centrifugal precipitates with cyclohexane.

Yb(OA)$_3$ preparation

A mixed solution of HOA/ODE (3.6 mL/9 mL) was added to a 50 mL flask containing 0.6 mmol of Yb(CH$_3$COO)$_3$. Then, the reaction system was heated at 160 °C for 30 min to obtain Yb(OA)$_3$. The as-formed Yb(OA)$_3$ was collected *via* centrifugation after addition of ethanol (14 000 rpm, 5 min).

Monitoring of the nucleation reactions in NaOA-based solvothermal controlled synthesis of NaYbF$_4$:Er UCNCs

The NaOA-based solvothermal UCNC synthesis reactions were stopped immediately after the system reached the pre-determined temperature, followed by rapid cooling down to room temperature with the help of cool air flow. The precipitate was collected by direct centrifugation or centrifugation after the addition of ethanol. Then, washing procedures were performed by re-dispersing the corresponding precipitate in cyclohexane, followed by the addition of ethanol, and centrifugation.

Seed-mediated epitaxial growth of NaYF$_4$ onto β-NaYbF$_4$:Gd/Er

A shell of NaYF$_4$ was grown onto the β-NaYbF$_4$:Gd/Er UCNCs by using procedures based on the conventional seed-mediated epitaxial growth strategy.[17]

Preparation of β-NaYbF$_4$:Gd/Er by using a nano-sized NaF-based solvothermal strategy

The β-NaYbF$_4$:Gd/Er was prepared according to the procedure reported in the literature.[10] Nano-sized NaF was formed by dissolving NaOH and NH$_4$F into methanol.[17] Following the literature, nano-sized NaF, instead of NaOA, was used as the source of the sodium supply.

Characterization

High-resolution transmission electron microscopy (HRTEM), high-angle annular dark-field (HAADF), element mapping and energy-dispersive X-ray analysis (EDXA) were performed using a Tecnai G^2 F20 microscope (FEI, USA). A D8 ADVANCE X-ray diffractometer (Bruker, Germany) with Cu Kα radiation (λ = 0.15418 nm) was used to collect XRD patterns. Upconversion luminescence spectra of the different samples were collected using a RF-5301 spectrofluorometer (Shimadzu, Japan). The samples were excited by a 980 nm laser source.

Results and discussion

Tuning the NH_4F/RE ratio in the vicinity of the stoichiometric value had a significant effect on the NC size in the NaOA-based solvothermal $NaYbF_4$:Er synthesis. As reported previously, a conventional stoichiometric ratio of NH_4F/RE (4 : 1) provided β-$NaYbF_4$:Er particles with an average diameter of 11.0 nm ± 6.5% by reacting at 300 °C for 20 min.[17] In this work, we found that a slight increase in the NH_4F/RE ratio from 4 : 1 to 4.25 : 1 provided monodisperse and smaller β-$NaYbF_4$:Er particles (10.5 nm, Fig. S1A†), showing an attractive NC diameter decrease effect.

Therefore, fine-tuning of the NH_4F/RE ratio (4.5 : 1, 4.75 : 1 and 5 : 1) was carried out to explore the possibility of achieving sub-10 nm β-$NaYbF_4$:Er. The NC diameter showed a decreasing and then an increasing tendency with an increased NH_4F/RE ratio, and sub-10 nm narrowly size-distributed β-$NaYbF_4$:Er (9.5 nm ± 5.6%) was obtained at the NH_4F/RE ratio of 4.5 : 1 (Fig. 1A–D, S1†). The peak width evolution of the as-prepared β-$NaYbF_4$:Er in the XRD pattern results was in agreement with the NC diameter variation tendency (Fig. S2†). Encouragingly, the use of precise modification of the NH_4F/RE ratio overcame the issue of controlled synthesis of sub-10 nm monodisperse β-$NaYbF_4$:Er. Notably, the optimal NH_4F/RE ratio differed from the conventional optimal ratio of 4 : 1.

To reveal the origin of the above sensitive dependence of the $NaYbF_4$:Er growth characteristics on the fluoride level, further investigations of the UCNC growth characteristics under different $NaOA/NH_4F/RE$ ratios were performed (Table 1). An even higher NH_4F/RE ratio of 6 : 1 provided α-, (α + β)- and β-$NaYbF_4$:Er by reacting at 300 °C for 20 min, 30 min and 45 min, respectively, showing a definite delayed phase transition (Fig. S3†). The diameter of the β-$NaYbF_4$:Er particles obtained

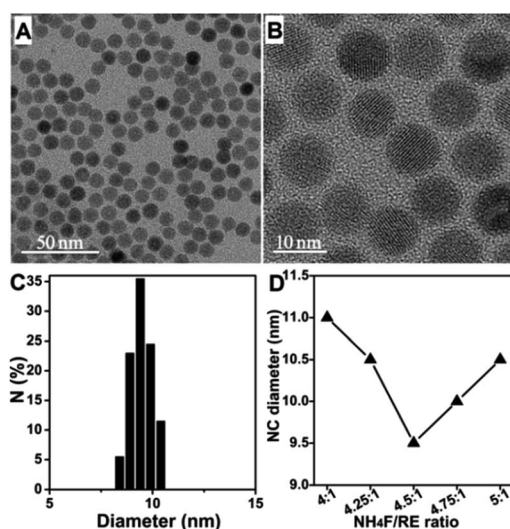**Table 1** Monitoring of the α-to-β transition process of $NaYbF_4$:Er under different $NaOA/NH_4F/RE$ ratios

$NaOA/NH_4F/RE$ ratio	20 min	30 min	45 min
2.5 : 6 : 1	α	α + β	β
2.5 : 3.5 : 1	α	α	α + β
1.9 : 4.5 : 1	α + β	β	
3 : 6 : 1	α	α + β	β

by using a higher NH_4F/RE ratio (6 : 1) was much larger than that of the particles obtained by using a lower NH_4F/RE ratio (49.6 nm ± 4.5%, Fig. 2A *vs.* Fig. 1A).

The formation of larger β-UCNCs under a much higher fluoride level may be attributed to the high surface coverage of F^- ions on the NCs according to the theory proposed by Gao *et al.*[19] It is possible that a universal and clearer NC nucleation theory could be established to render this F^- ion coverage theory compatible with the abovementioned α-nuclei sodium abundance theory[15] and thus supply useful guidelines for solvothermal UCNC controlled synthesis.

The important role of the sodium and fluoride levels in the solvothermal UCNC growth suggested that the *in situ* NaF generation reaction may have significant effects on the NC nucleation and growth. First, the system NaF levels were monitored after reacting at 300 °C for 0 min in the NaOA-based $NaYbF_4$:Er synthesis system. Since the α-to-β transition of $NaYbF_4$:Er was difficult, α-nuclei and NaF were collected at this stage. The mass of the collected NaF was 3.9 mg, 12.2 mg and 25.0 mg when the $NaOA/NH_4F/RE$ ratio was 2.5 : 4 : 1, 2.5 : 4.5 : 1 and 2.5 : 6 : 1, respectively, showing an obvious tendency of increasing with increased NH_4F/RE ratio (Fig. 2B). Therefore, the actual sodium and fluoride source, which could participate in the α-nuclei formation rather than in the inert NaF generation, supplied effective $NaOA/NH_4F/RE$ ratios of 2.35 : 3.85 : 1, 2.02 : 4.02 : 1 and 1.5 : 5 : 1 for the used $NaOA/NH_4F/RE$ ratios of 2.5 : 4 : 1, 2.5 : 4.5 : 1 and 2.5 : 6 : 1, respectively (Fig. 2B). A significant amount of sodium/fluoride participated in NaF generation rather than in UCNC nucleation, and we therefore can suggest that the larger β-$NaYbF_4$:Er

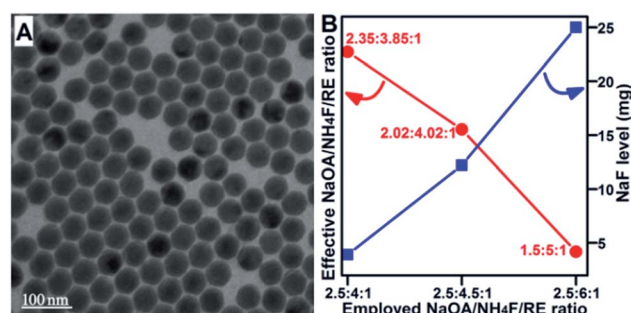**Fig. 1** TEM (A) and HRTEM image (B) of β-$NaYbF_4$:Er prepared by using a NaOA-based solvothermal strategy with an NH_4F/RE ratio of 4.5 : 1 (NC growth was carried out at 300 °C for 20 min). (C) Size distribution of the NCs shown in (A). (D) Plot of NC size against the NH_4F/RE ratio used for β-$NaYbF_4$:Er.

Fig. 2 (A) TEM image of β-$NaYbF_4$:Er prepared by using a NaOA/NH_4F/RE ratio of 2.5 : 6 : 1. (B) Plot of effective $NaOA/NH_4F/RE$ ratio and system NaF level *versus* used $NaOA/NH_4F/RE$ ratio after reacting at 300 °C for 0 min in the NaOA-based solvothermal $NaYbF_4$:Er synthesis system.

particles obtained at low and high NH_4F/RE ratios were due to the formation of fluoride-deficient and sodium-deficient α-nuclei formation environments, respectively. The sodium-deficient environment under a high NH_4F/RE ratio (*e.g.*, 6 : 1) should supply sodium-deficient α-nuclei, and thus, the formation of larger β-UCNCs could be supported by the sodium content-dependent α-to-β transition characteristics of α-UCNCs reported in the literature.[15]

Interestingly, sub-10 nm β-NaYbF$_4$:Er was achieved at the effective and nearly stoichiometric NH_4F/RE ratio of 4.02 : 1, which was realized by compensating the system fluoride consumption in the NaF generation reaction *via* a slight NH_4F dosage increase (Fig. 1A and 2B). In fact, the classic NaOA/NH_4F/RE ratio of 2.5 : 4 : 1 supplied a fluoride-deficient nucleation environment for the preparation of β-NaYbF$_4$:Er. The reactivity between sodium and fluoride was strengthened under elevated temperatures, leading to the competing and unfavorable NaF generation reaction during nucleation. The *in situ* NaF generation reaction competes with the α-nuclei formation reaction in consuming both sodium and fluoride sources during nucleation. Further monitoring of the α-nuclei formation process supported the effects of the competing NaF generation reaction (Fig. 3).

No NaF could be observed in the optimized NH_4F/RE ratio (4.5 : 1)-based solvothermal NaYbF$_4$:Er synthesis system (reaction at 160 °C, 0 min) *via* direct centrifugation, and only rare-earth oleates and α-nuclei were obtained *via* centrifugation after the addition of ethanol in such a system (Fig. 3A–C, S4†). In contrast, a large amount of precipitate was obtained in a high NH_4F/RE ratio (6 : 1)-based solvothermal system (reacting at 160 °C, 0 min) *via* direct centrifugation (Fig. S4†). The obtained XRD

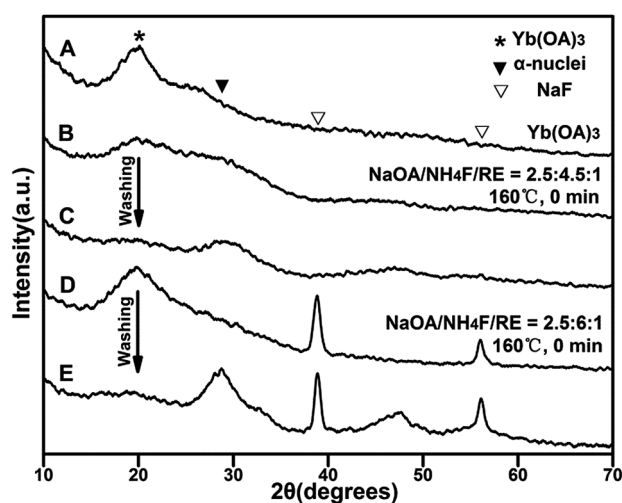patterns indicated that this precipitate was a mixture of rare-earth oleates, NaF and α-nuclei (Fig. 3A, D and E). The formation of rare-earth oleates with low dispersity should be due to the excessive surface binding of F$^-$ ions on the oleates under a high NH_4F/RE ratio. The excessive surface binding of F$^-$ ions onto rare-earth oleates not only strengthened the NaF generation reaction, but also retarded the formation of monodisperse α-nuclei, as well as the α-to-β transition, by consuming the active sodium source of the system. These results confirmed the importance of the competing *in situ* NaF generation reaction for UCNC nucleation.

The effects of the competing NaF generation reaction on UCNC nucleation were also verified by the NC evolution characteristics under fluoride- or sodium-deficient environments. The NaOA/NH_4F/RE ratio of 2.5 : 3.5 : 1 provided (α + β)-NaYbF$_4$:Er even after reacting at 300 °C for 45 min, but large β-UCNCs had already appeared (Fig. 4A, S5,† Table 1), indicating that insufficient system fluoride actually retarded the UCNC α-to-β transition.

To further show the sensitive effect of fluoride level variation on the NC size evolution, we attempted to prepare NaYbF$_4$:Er by partial fluoride consumption by slightly elevating the NaOA dosage (NaOA/NH_4F/RE, 2.75 : 4.5 : 1) and strengthening NaF generation. Approximately 20.6 mg of NaF was collected in the NaOA-based solvothermal system after reacting at 300 °C for 0 min. The intrinsic and effective NaOA/NH_4F/RE ratio for α-nuclei formation was thus only 1.93 : 3.68 : 1 for the used NaOA/NH_4F/RE ratio of 2.75 : 4.5 : 1, which supplied an obvious fluoride-deficient nucleation environment. Compared to the β-NaYbF$_4$:Er obtained by using the NaOA/NH_4F/RE ratio of 2.5 : 4.5 : 1, the expected much larger β-NaYbF$_4$:Er particles (13.4 nm $\pm$ 5.9%) were obtained after reacting at 300 °C for 20 min (Fig. 4B).

Fig. 3 XRD patterns: (A) Yb(OA)$_3$; (B) the precipitate collected *via* only a single centrifugation after the addition of ethanol for the NaOA-based NaYbF$_4$:Er synthesis system (NaOA/NH$_4$F/RE, 2.5 : 4.5 : 1, 160 °C, 0 min); (C) the product collected after a single washing procedure for the precipitate used in (B); (D) the precipitate collected *via* direct centrifugation for the NaOA-based NaYbF$_4$:Er synthesis system (NaOA/NH$_4$F/RE, 2.5 : 6 : 1, 160 °C, 0 min); (E) the precipitate collected *via* a single centrifugation after the addition of ethanol and a single washing procedure for the reaction solution used in (D).

Fig. 4 TEM images of NaYbF$_4$:Er prepared by using different NaOA/NH$_4$F/RE ratios: (A) 2.5 : 3.5 : 1; (B) 2.75 : 4.5 : 1; (C) 1.9 : 4.5 : 1; (D) 3 : 6 : 1. The NC growth reactions were performed at 300 °C for (A and D) 45 min or (B and C) 20 min.

A slight active sodium deficiency of the system also led to a significantly delayed α-to-β transition process for NaYbF$_4$:Er (Fig. S6,† Table 1). The α-to-β transition was finished after reacting at 300 °C for 30 min rather than 20 min by using the sodium-deficient NaOA/NH$_4$F/RE ratio of 1.9 : 4.5 : 1. Such sodium deficiency led to larger-sized β-NaYbF$_4$:Er particles (11.5 nm ± 6.3%, Fig. 4C). The α-to-β transition of NaYbF$_4$:Er was still not finished after reacting at 300 °C for 30 min under an even more severe sodium-deficient environment (NaOA/NH$_4$F/RE, 1.5 : 4.5 : 1), whereas larger β-NaYbF$_4$:Er particles with an average diameter of ∼15.0 nm had emerged (Fig. S7†). These results were in agreement with the hypothesis of sodium-deficient α-nuclei for the formation of larger UCNCs and delayed α-to-β transition under high NH$_4$F/RE ratios.[15] The system sodium and fluoride levels played cooperative roles in regulating the effective sodium-fluoride levels during the nucleation.

The NaF consumption process of the system also supported the important role of the competing NaF generation reaction during the nucleation for the UCNC evolutions. Considerable NaF (∼15.0 mg) still existed even after reacting at 300 °C for 20 min when using the NH$_4$F/RE ratio of 6 : 1, while there was no obvious NaF collected when using a lower NH$_4$F/RE ratio (e.g., 4 : 1, 4.5 : 1). It should be mentioned that the UCNC growth reaction of NaF + ReF$_3$ + mβ-UCNCs (small) → β-UCNCs proposed by Ju and co-worker supported the NaF-dependent β-UCNC growth characteristics described in our work.[20] In other words, larger-sized β-UCNCs would be formed when abundant NaF existed and was consumed at the NC growth stage.

Another attempt to improve the amount of active sodium source in the solvothermal system by raising the NaOA dosage (NaOA/NH$_4$F/RE, 3 : 6 : 1) also failed to achieve a better α-to-β transition environment and smaller-sized β-NaYbF$_4$:Er (57.3 ± 4.5%, Fig. 4D, S8,† Table 1). The mass of NaF collected after reacting at 300 °C for 20 min was ∼25.5 mg, indicating that the newly added NaOA could not supply as effective an active sodium source for NC nucleation because most of it was consumed in promoting the NaF generation reaction by reacting with the active fluoride in the system instead. The active sodium level of the system was constrained by the NaF generation reaction and thus could not be promoted by a simple increase of the dosage.

In summary, the origin and mechanism of the competing NaF generation and α-nuclei formation reactions in the solvothermal β-NaYbF$_4$:Er synthesis could be described as follows. (i) An in situ NaF generation reaction occurs between the sodium and fluoride sources during the system temperature increase, leading to consumption of both sodium and fluoride in the system. (ii) Since α-nuclei are formed by consuming the rare-earth oleates in the system, the sodium and fluoride sources reached the predetermined UCNC growth temperature (e.g., 300 °C) first, and the in situ NaF generation reaction competes with α-nuclei formation in the consumption of sodium and fluoride sources during α-nucleation. (iii) The effective system sodium-fluoride sources, which participate in α-nucleation rather than in in situ NaF generation, should determine the α-nucleation efficiency. For instance, the

effective NaOA/NH$_4$F/RE ratio for α-nucleation was only 1.93 : 3.68 : 1 for the used NaOA/NH$_4$F/RE ratio of 2.75 : 4.5 : 1 because the sodium-fluoride sources of the system were consumed in part by the in situ NaF generation reaction, resulting in low α-nucleation efficiency because the effective system fluoride level is lower than the necessary stoichiometric value. Briefly, the excessive system sodium source consumes the fluoride source via the in situ NaF generation reaction and thus leads to fluoride-deficient α-nucleation, and vice versa. (iv) The α-nucleation efficiency is positively related to the amount of β-nuclei formed at the UCNC growth temperature and therefore is inversely related to the size of the final β-NCs.

The findings of the competing in situ NaF generation reaction and α-nucleation are also in agreement with the thermodynamically controlled UCNC α-to-β phase transition mechanism. As is well known, a higher UCNC growth temperature will facilitate the transformation from metastable α-nuclei to the thermodynamically stable β-nuclei. The intrinsic reason for the accelerated α-to-β phase transition under higher temperature should be the promoted reactivity of the involved ions (Re^{3+}, Na$^+$, and F$^-$) and the resultant easier lattice modulation and rearrangement. In other words, the low reactivity of the involved ions would retard the UCNC α-to-β phase transition. NaF generation balance exists in the solvothermal β-NaYbF$_4$:Er synthesis system, including the in situ NaF generation at low temperature α-nucleation and NaF consumption at high temperature β-nucleation/growth. Excessive in situ generated NaF will not only lead to a low α-nucleation efficiency, but also to a low reactivity of the Na$^+$ and F$^-$ ions because of the inertness of NaF. Most of the in situ generated inert NaF would contribute to the later β-nuclei growth period rather than the initial β-nuclei formation period, leading to fewer β-nuclei, delayed α-to-β transition and larger β-NCs.

After overcoming the issue of facile control of the synthesis of sub-10 nm monodisperse β-NaYbF$_4$:Er and revealing the competing reactions during the nucleation process, low-level Gd^{3+}-doped (10%) β-NaYbF$_4$:Er was prepared according to this strategy. The diameter of the β-NaYbF$_4$:Er particles decreased from 9.5 nm ± 5.6% to 5.7 nm ± 7.8% after doping of 10% Gd^{3+}, showing an impressive size decrease effect (Fig. 5A). The diameter of 5.7 nm is in sharp contrast to the much larger diameter of NaYbF$_4$:Gd/Tm particles (10/0.5%) (∼80 nm) prepared by using a much longer reaction time (1.5 h) and a nano-sized NaF-based solvothermal strategy.[9]

Monodisperse β-NaYbF$_4$:Gd/Er (10/2%) was also achieved by using an even shorter reaction time of 15 min under the optimized NC synthesis conditions for 9.5 nm β-NaYbF$_4$:Er (Fig. 5B and C, 5.5 nm ± 6.9%). In fact, the NC size distribution was more narrow than that of the NCs prepared using the reaction time of 20 min as seen from the comparison of Fig. 5A and B, indicating the presence of NC Ostwald-ripening if the solvothermal reaction was not stopped in time. Gd^{3+} doping resulted in an earlier appearance of the Ostwald-ripening phenomenon for β-NaYbF$_4$. Elemental analysis showed that the actual Gd^{3+}-to-Yb^{3+} ratio in the as-prepared β-NaYbF$_4$:Gd/Er (10/2%) was ∼1 : 9.2, very close to the theoretical value (1 : 8.8), indicating the successful Gd^{3+} doping into β-NaYbF$_4$ (Fig. 5D–F,
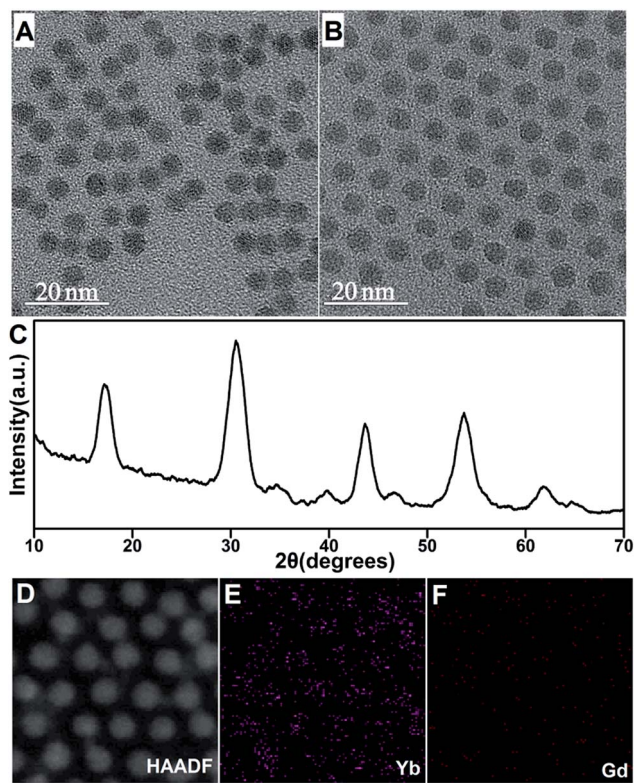
Fig. 5 TEM images of β-NaYbF$_4$:Gd/Er (10/2%) prepared using the optimized NC synthesis conditions for 9.5 nm β-NaYbF$_4$:Er and reacting at 300 °C for 20 min (A) and 15 min (B). (C) Corresponding XRD pattern of the sample used in (B). (D) HAADF image of randomly selected NCs for the sample used in (B). (E and F) Element maps for the NCs shown in (D).

S9†). These results demonstrated that balancing the competing NaF generation and α-nuclei formation reactions successfully overcame the challenge of the controlled solvothermal synthesis of sub-10 nm low-level Gd^{3+}-doped β-NaYbF$_4$:Er.

For control experiments, NaYbF$_4$:Gd/Er (10/2%) was prepared according to the nano-sized NaF-based solvothermal strategy reported in the literature.[10] The α-to-β transition was still not completed after 40 min of reaction at 300 °C (Fig. 6A). Pure β-UCNCs as large as ~70 nm were achieved after reacting at 300 °C for 60 min (Fig. 6B). Moreover, the as-prepared β-
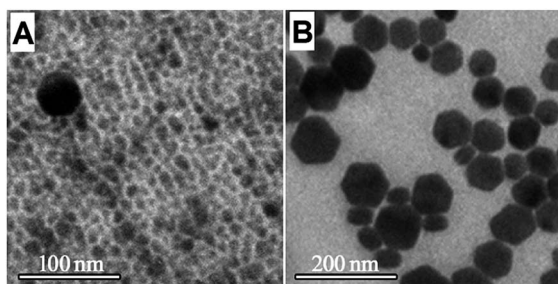

Fig. 6 TEM images: NaYbF$_4$:Gd/Er (10/2%) prepared by using the nano-sized NaF-based solvothermal strategy and reacting at 300 °C for 40 min (A) and 60 min (B).

UCNCs are very non-uniform in morphology. This phenomenon is not caused by the Ostwald-ripening mechanism because the α-to-β transition has just finished. The β-nuclei for β-UCNCs with sharp size differences should form in different nucleation periods, which could be explained by the slow release of the Na$^+$ and F$^-$ ions from the inert nano-sized NaF. These comparisons confirmed that low-level Gd^{3+} doping could not obtain sub-10 nm β-UCNCs using the nano-sized NaF-based solvothermal strategy due to *ex situ* NaOH/NH$_4$F-to-inert NaF conversion. The UCNCs prepared *via* the nano-sized NaF-based strategy were still too large for bio-applications (Fig. 6B).

Finally, the upconversion intensity of the as-prepared 5.5 nm β-NaYbF$_4$:Gd/Er (10/2%) was evaluated by comparison to high-level (40%) Gd^{3+}-doped β-NaYbF$_4$:Er, as well as the large-sized β-NaYbF$_4$:Gd/Er (30/2%) with promising upconversion efficiency for practical applications. Similar-sized β-NaYbF$_4$:Gd/Er (40/2%) (~5.6 nm) was achieved by using the same synthesis procedures as those of the 5.5 nm β-NaYbF$_4$:Gd/Er (10/2%) (Fig. S10A†). The low-level Gd^{3+}-doped β-NaYbF$_4$:/Er showed a stronger upconversion intensity than the high-level Gd^{3+}-doped NaYbF$_4$:/Er, suggesting that the NaYbF$_4$ may be a more efficient upconversion host material than NaGdF$_4$ (Fig. S10D†). Our previous work also supports the conclusion that NaYbF$_4$ is an excellent upconversion host material.[17] However, the upconversion intensity of the 5.5 nm β-NaYbF$_4$:Gd/Er (10/2%) is much weaker than that of the large-sized β-NaYbF$_4$:Gd/Er (30/2%) (~20 nm, Fig. S10B†) obtained using the procedure based on the reports in the literature.[10] In view of the much higher surface-to-volume ratio of the smaller-sized β-NaYbF$_4$:Gd/Er and the resultant low upconversion intensity induced by surface quenchers, an optically inert NaYF$_4$ shell was coated onto β-NaYbF$_4$:Gd/Er (10/2%) for upconversion intensity strengthening. The upconversion intensity of the as-obtained small-sized core/shell structured β-NaYbF$_4$:Gd/Er(10/2%) @NaYF$_4$ (~9 nm, Fig. S10C†) is comparable to that of the literature-based large-sized β-NaYbF$_4$:Gd/Er (30/2%), indicating the potential of the as-obtained low-level Gd^{3+}-doped β-NaYbF$_4$:Er for practical application (Fig. S10E†).

Conclusions

We showed that the effective sodium-fluoride levels for α-nuclei formation were restricted sensitively by the competing *in situ* NaF generation reaction in NaOA-based solvothermal UCNC synthesis. The effects of the sodium and fluoride levels on the solvothermal UCNC evolution have been partially neglected in the respective F$^-$ ion coverage and the α-nuclei sodium abundance theories discussed in the literature.[15,19] The competing NaF generation and α-nuclei formation reactions were the theoretical basis for both the F$^-$ ion coverage and the α-nuclei sodium abundance theories. Sub-10 nm monodisperse β-NaYbF$_4$:Er (9.5 nm) and low-level Gd^{3+}-doped (10 mol%) β-NaYbF$_4$:Er (5.5 nm) were achieved *via* facile balancing of the competing *in situ* NaF generation and α-nuclei formation in the absence of high NaOA and NH$_4$F dosages. Our work supplies new insights and a user-friendly tool for the control of solvothermal UCNC synthesis.

Conflicts of interest

There are no conflicts of interest to declare.

Acknowledgements

References

1 N. M. Idris, M. K. G. Jayakumar, A. Bansal and Y. Zhang, *Chem. Soc. Rev.*, 2015, **44**, 1449–1478.

2 X. G. Liu, C. H. Yan and J. A. Capobianco, *Chem. Soc. Rev.*, 2015, **44**, 1299–1301.

3 D. L. Zhou, D. L. Liu, W. Xu, X. Chen, Z. Yin, X. Bai, B. Dong, L. Xu and H. W. Song, *Chem. Mater.*, 2017, **29**, 6799–6809.

4 G. Y. Chen, H. L. Qju, P. N. Prasad and X. Y. Chen, *Chem. Rev.*, 2014, **114**, 5161–5214.

5 Q. S. Chen, X. J. Xie, B. L. Huang, L. L. Liang, S. Y. Han, Z. G. Yi, Y. Wang, Y. Li, D. Y. Fan, L. Huang and X. G. Liu, *Angew. Chem., Int. Ed.*, 2017, **56**, 7605–7609.

6 H. X. Mai, Y. W. Zhang, R. Si, Z. G. Yan, L. D. Sun, L. P. You and C. H. Yan, *J. Am. Chem. Soc.*, 2006, **128**, 6426–6436.

7 F. Shi and Y. Zhao, *J. Mater. Chem. C*, 2014, **2**, 2198–2203.

8 Q. Liu, Y. Sun, T. S. Yang, W. Feng, C. G. Li and F. Y. Li, *J. Am. Chem. Soc.*, 2011, **133**, 17122–17125.

9 J. A. Damasco, G. Y. Chen, W. Shao, H. Agren, H. Y. Huang, W. T. Song, J. F. Lovell and P. N. Prasad, *ACS Appl. Mater. Interfaces*, 2014, **6**, 13884–13893.

10 Y. L. Liu, K. L. Ai, J. H. Liu, Q. H. Yuan, Y. Y. He and L. H. Lu, *Angew. Chem., Int. Ed.*, 2012, **51**, 1437–1442.

11 Z. Q. Li and Y. Zhang, *Nanotechnology*, 2008, **19**, 345606.

12 C. S. Ma, X. X. Xu, F. Wang, Z. G. Zhou, S. H. Wen, D. M. Liu, J. H. Fang, C. I. Lang and D. Y. Jin, *J. Phys. Chem. Lett.*, 2016, **7**, 3252–3258.

13 D. D. Li, Q. Y. Shao, Y. Dong and J. Q. Jiang, *Chem. Commun.*, 2014, **50**, 15316–15318.

14 T. Rinkel, A. N. Raj, S. Duhnen and M. Haase, *Angew. Chem., Int. Ed.*, 2016, **55**, 1164–1167.

15 T. Rinkel, J. Nordmann, A. N. Raj and M. Haase, *Nanoscale*, 2014, **6**, 14523–14530.

16 R. K. Shi, M. A. Ling, X. N. Li, L. Zhang, M. Lu, X. J. Xie, L. Huang and W. Huang, *Nanoscale*, 2017, **9**, 13739–13746.

17 J. W. Shen, Z. Q. Wang, J. W. Liu and H. Li, *J. Mater. Chem. C*, 2017, **5**, 9579–9587.

18 L. Q. Xiong, T. S. Yang, Y. Yang, C. J. Xu and F. Y. Li, *Biomaterials*, 2010, **31**, 7078–7085.

19 C. Y. Liu, Z. Y. Gao, J. F. Zeng, Y. Hou, F. Fang, Y. L. Li, R. R. Qiao, L. Shen, H. Lei, W. S. Yang and M. Y. Gao, *ACS Nano*, 2013, **7**, 7227–7240.

20 J. N. Shan and Y. G. Ju, *Nanotechnology*, 2009, **20**, 275603.